Correlation Between Microstructural And Mechanical Properties In Niobium Carbide Reinforced Hadfield Steel Composites

Lakshmi Manogna Dama

LUTMDN/(TMMV-5326)/1-47/2021

2021

LUND UNIVERSITY

LTH
FACULTY OF ENGINEERING

MASTER THESIS
DIVISION OF PRODUCTION AND MATERIALS ENGINEERING
LUND UNIVERSITY

University Supervisor : Latifa Melk, Adjunct lecturer
Examiner: Jan Eric Stähl

Author: Lakshmi Manogna Dama
Lund, Sweden 2021

Avdelningen för Industriell Produktion
Lunds Tekniska Högskola
Lunds universitet
Box 118
221 00 Lund
Sverige

Division of Production and Materials Engineering
LTH, School of Engineering
Lund University
Box 118
SE-221 00 Lund
Sweden

Printed in Sweden
Media-Tryck
Lund University

Acknowledgement

- To **Dr. Latifa Melk**, I appreciate the kind of dedication that she has towards her work and her students; I would like to thank her for giving me an excellent opportunity; her supervision and suggestions have always guided me towards the right direction and final gratitude for having trust in me that I would finish this project.
- To Dr. Andrii Hrechuk, thank you for helpful suggestions and assistance with the pressing machine.
- To Mikael Hörndahl, Ryszard Wierzbicki, Axel Bjerke and Klas Holger Jönsson special thanks to you all for helping me out with experimental equipment and cutting work.
- Thanks to Michael Hybelius, for his assistance in wear testing.
- Special thanks to Hema Kalidasu and Manideep Beri for constant support throughout the project, and thanks to Adam Johansson and Isac Lazar, it was great working with you all.
- Thanks to **Jan Eric Ståhl** and the entire department of Production and Materials Engineering who have helped me throughout my thesis.

Lakshmi Manogna Dama
2021-06-14
Lund, Sweden

Abstract

Degradation of tools is a prevalent aspect in the mechanical world; due to the advancement of technologies and intense research and development, there are new ways and ideas to curb or delay the tool failures; one such idea is to implement Metal Matrix Composites (MMCs) with various reinforcement materials. This thesis focuses on improving the hardness and wear resistance of Hadfield steel by reinforcing it with Niobium Carbide (NbC).

This whole project is categorized into three sections, beginning with literature study, implementing theory into practice by reinforcing NbC into Hadfield steels, and later investigating the microstructural results by material characterization techniques like Scanning Electron Microscopy (SEM) followed by wear testing.

This study involves the investigation of microstructure and hardness. The ultimate result from this thesis is determining the suitable NbC material to reinforce Hadfield steel, and the results have shown that the hardness has increased in the studied test samples.

Keywords: Metal Matrix Composites (MMCs), Hadfield steels, Reinforcement.

Table of Content

List of Figures

List of tables

1. Introduction

1.1. Background

The need for desired properties keeps varying depending upon the application of the material. To meet today's mechanical world demands, the materials should possess properties that increase their potential to perform efficiently with improved longevity. Over the past two decades, there has been strong inclination towards the usage of composites in many fields like aerospace, architecture, automotive, energy, etc. With this increasing demand, several improvements and advancements are made in composites, like developing various reinforcing techniques, introducing various reinforcing materials, etc.

Metal Matrix Composites (MMCs) are one of the most commonly used composites for various applications. The MMCs combine matrix material properties with the properties of the reinforcements used, resulting in a material with desired properties. In this project, Niobium carbide is utilized to reinforce Hadfield steel, to improve its hardness and wear resistance.

1.2. Objectives of the thesis

This project begins with an introduction to MMC and discusses in particular concerning NbC; this project involves theoretical derivations followed by experimental analysis of NbC in Hadfield steel. A detailed microstructural analysis is performed and is correlated with hardness of the samples. The project's ultimate goal is to find out the best suitable sample to be used as a reinforcement that satisfies the wear test results.

2. Literature Review

2.1. Metal Matrix Composites

2.1.1. General

As the name suggests, Metal Matrix Composites (MMC) consist of at least two chemically and physically distinct phases, which combine to obtain properties absent in the individual phase [1] [1]. MMCs have historical significance as they were produced as layered structures using combinations of metallic and non-metallic constituents but gained significant importance as engineering composite materials in the second half of the twentieth century [1]. The primary means of producing MMCs used energy-intensive manual tasks such as hammering and applying laminations. With the growing demands to assert world dominance and to ease geographical accessibility across the globe, MMCs began to be used in military and aerospace applications extensively. To do so, MMCs were produced using modern techniques, which included dispersing reinforcing agents into the matrix (Steels). Usually, the base metals in the matrix are low in density, for example, Aluminium [2].

The mechanical properties of the MMC will only improve when the base metal in combination with the reinforcement complement each other. Hence, it is essential to determine the correct blending parameters to yield the best results [1]. MMCs, when compared to unreinforced metals, have a greater specific strength, stiffness, operating temperature, wear resistance, almost zero coefficient of thermal expansion. While there are drawbacks such as high fabrication costs, low ductility, and low toughness, opening the scope for development in reinforcing techniques [3]. Unlike conventional alloys, metal matrix composites have multiple levels of matrix strengthening, including major alloying elements of the matrix alloy, as well as exogenous and endogenous reinforcing particles [4].
MMCs, when classified based on the reinforcement continuity, can be differentiated as particulate, whisker, and short fiber reinforcements, and

continuous fiber reinforcements based on their aspect ratio and diameter (Table 1) [1] [2]. On the other hand, composite matrices are classified into three categories based on the nature of the reinforcing agent, namely, Ceramic Matrix Composites (CMC), Metal Matrix Composites (MMC), and Polymer Matrix Composites (PMC). MMCs are considered advantageous when compared to CMCs and PMCs.

The MMCs have the following advantages over PMCs and CMCs [1] [6].

- Improved Service Temperature
- Improved Electrical and Thermal Conductivity
- Higher Strength and Strength
- Better Transverse Properties.
- Improved Joining characteristics
- Little or No contamination
- Better Process-ability
- Less moisture absorption
- Higher resistance to fire

Table 1: Basic MMC classification [1]

Type	Aspect ratio	Diameter, μm	Examples
Particle	1-4	1-25	SiC, Al_2O_3, BN, B_4C, WC
Short fiber or whisker	10-10000	1-5	C, SiC, Al_2O_3, Al_2O_3+SiO_2
Continuous fibre	>1000	3-150	SiC, Al_2O_3, C, B, W, Nb-Ti, Nb_3Sn

MMCs trail other metals and PMCs in technology maturity, challenging fabrication, and higher costs [6]. The section below will elaborate on the matrix and reinforcements in MMC.

2.1.2. Reinforcement

Generally, reinforcements are more substantial than the matrix in the composite. A sound reinforcement possesses properties such as [6] :

- Mechanical and Chemical compatibility
- Thermal Stability

- High Compression and Tensile Strength
- High Young's Modulus
- Financially efficient

Selection of reinforcement is often a challenging aspect as going wrong will lead to anomalies in the results. One must note that the difference between the size of the matrix powder and the reinforcement particle should be small for a uniform distribution, i.e., the reinforcement size should not be lesser than a critical value which is a function of matrix powder size and volume fraction and reduction ratio of the secondary processing (casting, extrusion, forging, etc). This is because the inter-particle size decreases with a decrease in reinforcement size and increased reinforcement volume fraction. The inter-particle spacing needs to be greater than the final transverse length of the matrix powders after secondary processing of the composite [7].
The approximate matrix percentage is determined by estimating the use of the composite material, and recent research has proposed the use of alloying theory to generalize the selection of reinforcements. However, the versatility in the reinforcements makes it hard for anyone to generalize a method to select and embed reinforcements. The reinforcements and nature of reinforcements metal composites are divided into particulate reinforced composites and fiber-reinforced composites. The fiber-reinforced composites are further classified into Continuous and Discontinuous fibers [1] [6].

2.1.2.1 Continuous Fibre Reinforcement

Continuous fiber reinforcements are those with minimum length to maximum transverse length ratio of the order 10:1, max cross-sectional area of 5.1x10-4cm2, and maximum transverse length of 0.0254cm. They are usually called filaments and are found in the form of monofilaments and multifilaments. Examples of this type of reinforcement are Boron, graphite, alumina, silicon carbide. Boron belongs to the family of monofilament fibers and is manufactured using CVD, whereas the rest mentioned in the list belong to multifilament and are found in the form of single yarns, two-or three-dimensional weaves [8] [9].

They can be classified into carbon and ceramic types. The carbon types mainly contain graphite, and the ceramic types consist of alumina, silica, Boron, alumina-silica, alumina-Boria-silica, zirconia, boron nitride, titanium diboride, silicon carbide, and boron carbide. It is essential to know that all these fibers are brittle, given their length (the strength decreases as the length increases) [10].

The reinforcements form coats on the matrix surface, which develop the bond strength of the composites by preventing undesirable reactions and diffusion due to the formation of reaction barriers, especially when the MMC is exposed to high-temperature processes. For example, the tensile strength of alumina can be enhanced after being reinforced with silica. A powerful bond between the fiber and matrix also can cause problems as it will lead to adhesion. Powerful adhesion bonds will mean the forces exerted on the fibers can propagate into the matrix material, making it brittle. To prevent this from happening, coatings have been practiced to act as a barrier and reduce the bond strength. In contrast, coatings can also increase the bond strength by promoting wetting if minimal bond strength maintains composite's functionality not obtained [10] [9].

The less common type of continuous fiber reinforcements is called wires which are metallic filaments. The wire-type reinforcements stand out due to their high elastic moduli, with molybdenum, beryllium, tungsten, and stainless steel being the commonly used wire reinforcements. These reinforcements are metallic and ductile; they are the preferred reinforcement choices for applications that need to withstand high tensile load and need to display a great deal of toughness [8] [1].

2.1.2.2 Discontinuous Fibre Reinforcement

Discontinuous fiber reinforcements can be categorized as particulate reinforcements and whisker reinforcements. Niobium carbide falls under the whisker type of reinforcement, while other carbides such as boron carbide, titanium carbide, and tungsten carbide are the other well-known

discontinuous reinforcements. Silicon carbide and boron carbide reinforcements are found even as particulate reinforcements [8] [1].

Studies suggest silicon carbide be the most commonly used whisker reinforcement. Whisker type reinforcements generally cost the most, and this can be exemplified using silicon carbide; the whisker form costs $95 per pound, whereas the particulate form costs just $3 per pound. This can be correlated to the higher costs associated with Niobium carbide reinforcement as the cost of 250g. Whisker-type reinforcements have a higher aspect ratio (L/d). However, they tend to break into shorter fragments during their processing making them weaker and brittle and difficult to pack, leading to random orientations during secondary processing. This can cause anisotropy which cannot be controlled easily. Difficulty in packing can be considered advantageous in conditions that require higher reinforcement to matrix ratio as they contribute to superior strength [11] [12].

Particulate Composite: This type of reinforcement is economically feasible and is growing in recognition. They contain a matrix reinforced by a dispersed phase in the form of ceramic particles. These composites are further classified based on the orientation of particles, i.e., random orientation and preferred orientation. Studies suggest that due to their isotropic property, they have great scope in structural applications [8] [6].
Graphite, SiC, SiO2, MgO, and ZrO2 are examples of ceramic particulate reinforcements; out of these, graphite has the highest tensile strength, making them capable of withstanding higher-order loads.

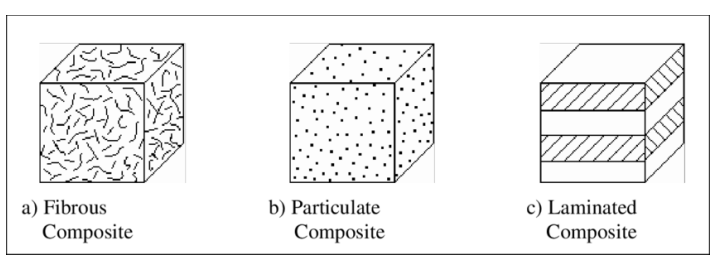

Figure 1: Represents variants in MMC based on particle type [13]

2.2 Reinforcement NbC

MMCs are ceramic-reinforced metals; these materials are metal-dominated, comprising a metal matrix containing ceramic particles to enhance their properties [15].

The most widely used ceramics for reinforcements are carbides, oxides, nitrides, borides. The commonly used carbides are TiC, WC, VC, NbC, etc., out of which W is a rare earth metal that makes its availability a difficulty, which justifies why W is expensive. TiC is much more complicated and has better wear resistance compared to WC, and also TiC is readily available and cheaper compared to WC, but TiC has poor toughness and poor wettability with its binder; however, several options of doping TiC with metals like Ni, Mo, Co helps in improving wettability issue in TiC.

NbC is generally employed as filaments in superconducting composites rather than as a matrix [16]. However, in recent years, NbC is widely used as a grain growth inhibitor in hard metals; this is basically by substituting Co with NbC, resulting in price reduction since Co is expensive [17]. The addition of NbC resulted in improved functional properties like an increase in fracture toughness and microhardness [17]. Generally, NbC is softer at room temperature than WC, but the stability of hot hardness for pure NBC is exceptional. NbC based MMCs are predominant these days in the automotive industry for disc brakes [18].

Compared with WC, VC, pure NbC has a melting point of 3600 celsius and high hardness of 19.6GPa, and the density of NbC is 7.82g/cm_3 [19] [20]. Steel's density varies depending on the alloying elements, though it typically falls between 7.75 and 8.05 g/cm 3, which is very close to the density of NbC. Considering the densities of WC and TiC from the table below, it is evident that their density differences concerning steel are relatively high, whereas NbC's density is almost in the range of the density of steel; this is a significant theory that should be discussed since the density of WC or TiC, or NbC should be relatively equivalent to the density of steel otherwise the WC/TiC particles will float or submerge in the molten steel. Thus, this could

result in a non-homogenously distributed MMC whose properties will not satisfy the critical need.

Table 2: Properties of various carbides [1] [21]

Main properties				
	NbC	**WC**	**TiC**	**ZrC**
Density	7.82g/cm_3	15.7g/cm_3	4.93g/cm_3	6.73g/cm_3
Youngs Modulus	450GPa	670-707 GPa	400GPa	440GPa
Shear Modulus	182GPa	262-298 GPa	188GPa	174GPa
Structure	Cubic F	HCC	FCC	Cubic crystal structure

2.3 Manufacturing methods

Manufacturing MMCs play a key role in determining the MMC's physical and mechanical properties. There are several MMC fabrication techniques; this is mainly due to the wide range of choice of material of reinforcement and the type of reinforcement needed. Hence, there is no specific tailor-made fabrication technique for MMCs as the manufacturers adapt to the customer's requirement and choose the best fabrication technique to produce the desired MMC. These steps are generally called primary and secondary processes [8].

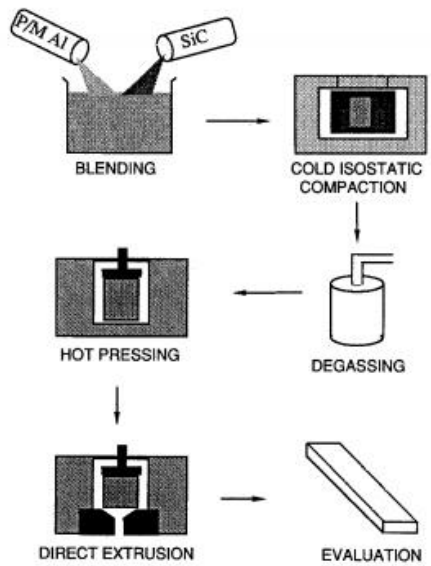

Figure 2: Example of Al, SiC blended together, where Al is matrix and SiC is the reinforcement [22]

The primary processes include mixing of the matrix-reinforcement loose particles through mechanical processes. The interacting ingredients are used in the form factor of powder, liquid metal, and solid fiber. The purpose behind the primary process is to obtain a homogenous mixture of the matrix-reinforcement preforms mainly. They are then compacted by applying pressure to undergo secondary processes [23] [11].

The secondary processes involve steps that energize particles and alter the microstructural capabilities of the MMC. Altering the microstructure (phases present) of the MMC enhances its mechanical properties and through processes such as heat-treatment, casting, extrusion, sintering). The major problem that is often encountered during the secondary processing is the material's inherent brittleness, which can worsen due to the high frictional forces imparted by the reinforcements [7] [11].

The processes to fabricate the MMC are classified based on the state of the raw ingredients in the pre-mixing phase. These classifications are (i) Solid-phase processes, (ii) Liquid-phase processes, (iii) deposition techniques [24].

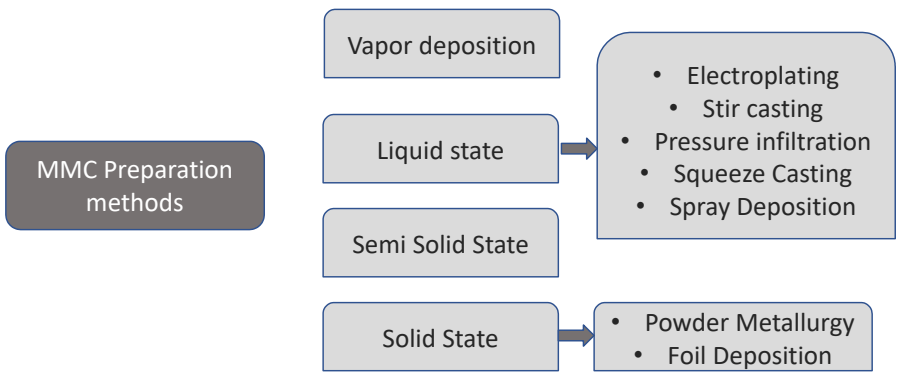

Figure 3: Represents various manufacturing methods of MMC [22]

2.3.1 Solid-State Processing

Solid-state processes utilize metal powder or foil as a matrix metal combined with particles or fibers as a state of reinforcements, i.e., discontinuous reinforcements. The reinforcements are infused in the metal matrix using diffusion techniques that employ high temperature and pressure, such as sintering. The solid-state processes include diffusion bonding, powder blending and consolidation, and physical vapor deposition.

Studies suggest Powder metallurgy as the most widely used technique to produce discontinuously reinforced MMCs. Here, the matrix materials are blended with the whisker or particulate reinforcement (ceramic fibers and particulates), which are then consolidated by either hot or cold pressing in the form of billets or slabs. The final MMCs are obtained by processes such as extrusion, rolling, or forging, which align the fibers of the matrix parallel to the direction of the applied force. These mechanical processes enhance the strength of the MMC while maintaining the homogeneity of the matrix-reinforcement blend.

A. Diffusion Bonding

The diffusion bonding method is a well-known sold state joining process with the first commercial application that dates back to the 1980s. It is a commonly used method for long processing time, high processing temperature, and pressure, making it a financially cumbersome process. In this method, similar or even dissimilar metals are joined by the interdiffusion of atoms at an elevated temperature and pressure between clean surfaces of metals in contact, which leads to the formation of bonds. This method is applicable for a wide variety of matrix metals, and they offer specific control over fiber orientation and volume fraction of the matrix [1].

A well-known variant of the diffusion method is the "foil-fiber-foil" process which involves a matrix alloy foil or a mixture of matrix powder and a fugitive organic binder and fiber arrays stacked in a predetermined order (cause for control over fiber orientation). These stacked layers are then hot pressed to trigger diffusion bonding [1].

One must keep in mind that the surfaces in contact must be machined to be as smooth as possible and maintained in an atmosphere free of chemical contaminants to prevent diffusion from occurring. The diffusion bonding occurs in stages, the first occurring even before the surfaces are entirely in contact. In this case, microscopic defects called asperities to come in contact and cause plastic deformation on a microscopic level. This gives rise to the formation of interfaces between the two surfaces of the metals. The high temperature and pressure accelerate the creep induced in the material, more specifically between grain boundaries and the diffusion of the material across the contact surfaces, leading to bond formation [1].

In regulating mechanical properties, fiber distribution is highly significant. In particular, fiber-to-fiber interaction or very close spacing between fibers can result in very high concentrations of localized tension, resulting in fiber cracking and matrix damage during processing, and under an applied load, premature damage, cracking, and composite failure [1].

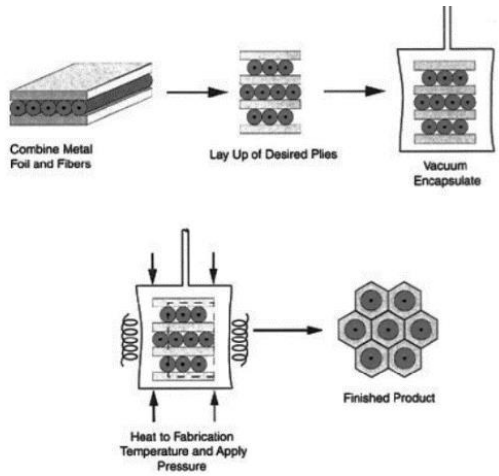

Figure 4: Schematic of diffusion bonding method [25]

B. Physical Vapor Deposition

The process of PVD is performed by evaporating the coating material under the influence of high energy. The fibers of the coating material go through a region of high partial vapor pressure for the application of reinforcement. This leads to the formation of vapors of the metal matrix when condensed, creates a coat on the surface of the fibers in the PVD chamber. The sources of high energy can vary from the electron beam to sputtering by magnetrons. In contrast, the vapor sources (for evaporation) can vary from resistance heating in a crucible, electron beam evaporation, arc evaporation, and radiation heating. The workpiece and the coating material are placed in a vacuum or a protective atmosphere (usually Argon gas is used to maintain an inert atmosphere) for the successful deposition of the coating. The bonds between the coating and the workpiece (target material) are formed when reactive gases such as Argon are flushed into the PVD chamber [26].

PVD is considered a prolonged process with a 5-10 micrometer deposition relatively minute, making it an energy-intensive process [24]. The PVD technique has more significant benefits when compared to other deposition techniques due to its ability to form/manufacture versatile samples and

unusual microstructures of the coating backed by excellent surface finish [27]. The internal stresses induced due to the process are known to increase towards the surface gradually. Hence the maximum value of the stresses is higher close to the edges of the composite resulting in clustering of compress stresses which leads to improvement in microhardness of the composite, which in turn improves its functional properties [28].

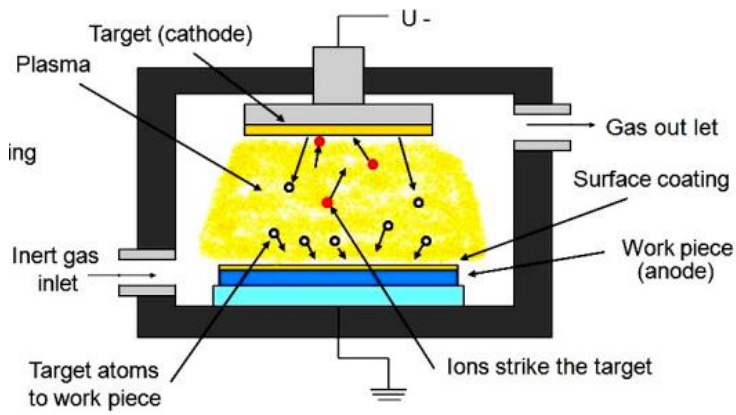

Figure 5: Schematic of physical vapour deposition [26]

2.3.2 Liquid State Processing

This group of MMC processing techniques involves incorporating the dispersed phase into a molten metal matrix which is then solidified. A high amount of wetting, i.e., good interfacial bonding between the dispersed and molten liquid phases, is required. This will be critical in giving a high level of mechanical ability [24]. Using liquid state processing comes with its advantages such as production of composites to near net shape, a faster rate of production, and the process associated with lower temperatures, thus making it less energy intensive compared to solid-state processing techniques [29].

Liquid state processing has several techniques but the most commonly used one's are Stir Casting, Liquid Metal infiltration, Squeeze casting and spray deposition, each of which has been explained below:

A. Stir Casting

Stir casting is a process where the composite is processed by adding a mixture of ceramic particulate reinforcement with a molten metal matrix. The reinforcement particulates are dispersed through high-energy mixing, which leads to the formation of slurry. The slurry is then compacted by casting into ingots or billets utilizing foundries, extrusion, or rolling the slurry. Achieving reinforcement particulate homogeneity is quite a challenge [30] [24].

Like most liquid state processes, it is essential to achieve good wettability between the reinforcement particles and the metal matrix; the addition of 1 wt% Mg can do this. At the same time, agglomeration tends to occur in reinforcements when the raw materials of the reinforcement particle exceeds to matrix ra wmaterials by 15%, which results in lower mechanical and tribological properties [29].

This process is considered most suitable for manufacturing composites with up to 30% vol—a fraction of reinforcement despite agglomeration. Stirring speed is an important process parameter; increasing it will lead to a higher level of uniform distribution, greater shear forces on the liquid metal, and increase Porosity. Parameters such as the velocity of stirring, angle of stirring, and stirring time are considered to control parameters for this process [31].

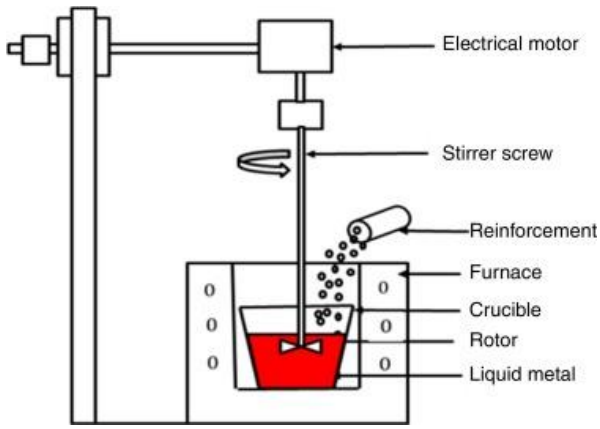

Figure 6: Schematic of stir casting equipment [32]

B. Squeeze casting

The squeeze casting method consists of pressure-assisted (forced) liquid infiltration of a fibrous or particulate preform, most suited for complex-shaped components or matrices that need localized reinforcements [8].

The molten metal is poured into the open die, after which the die is closed on the application of pressure of range (70-100Mpa) for the compaction of the melt. Hot air escapes the caste, lowering the temperature, thereby assisting in the solidification. Smaller size particles are usually beneficial due to their ability to provide more interfacial area, which serves as nucleation sites for grain formation (In practice, particle sizes of 20 micrometer and 40micrometer were analyzed for SiC and 20microm particle size should better reinforcement) [33].

Applying pressure to the solidification of molten metal may affect the melting point of the alloy, increasing the rate of solidification. Studies have been performed on stainless steel wire reinforced aluminum matrix composites fabricated by high-pressure squeeze-casting and showed that these composites at a 40% fiber volume fraction have a three times greater tensile strength than that of an aluminum matrix cast under the same fabrication conditions [34].

The process variables considered for squeeze casting are fiber and liquid preheat temperature, external cooling, the time lag between die- closure and pressurization, and the pressure levels should constantly be in check as imperfect control of these parameters leads to defects such as fiber degradation and oxide inclusion which weaken the composite [34].

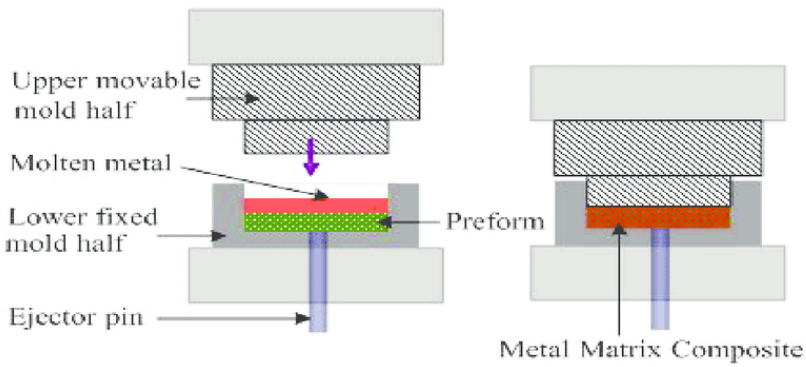

Figure 7: Schematic of squeeze casting [35]

C. Spray Co-deposition

Spray Co-deposition is a primary liquid processing technique for MMCs wherein the liquid metal is sprayed. The reinforcement (ceramic particles) are introduced to the spray stream, which yields a mixture of metal-reinforcement particles well-controlled environment. This mixture needs to be compacted using secondary mechanical processes such as hot-pressing, extrusion, and forging [1].

Composite monolayers, continuous and discontinuously reinforced composites can be fabricated using this method. This process improves high-cycle fatigue, creep behavior, thermal conductivity, and low service temperature.

This method has been used to develop AMCs using SiC as discontinuous reinforcement particles. Reinforcements of vol fraction up to 36% can be achieved using this method. However, this method fails to produce the best

reinforcements as it can face common challenges such as uniform distribution of reinforcement particles, oxygen contamination, selection of appropriate starting gas [27].

The decomposition layer created using this method has a porosity of 5-10% [24].

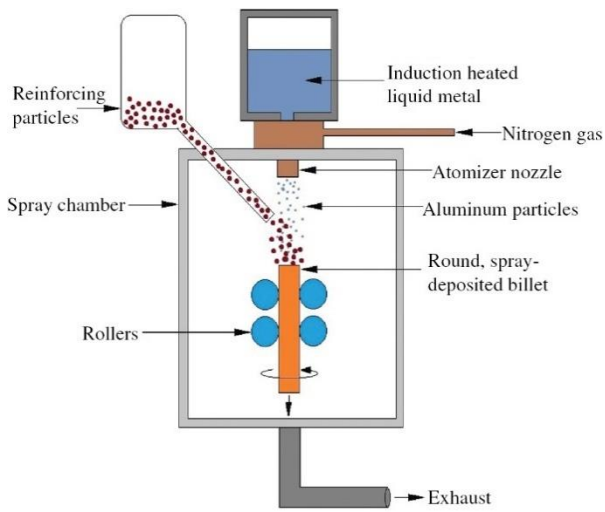

Figure 8: Schematic of spray deposition technique [36]

2.4 Manganese steel – The Matrix

Austenitic Manganese Steels are the family of steels that contain about 1-1.4 wt% Carbon and 10-14 wt% Manganese in their system. This group of Manganese steels are generally non-magnetic and possess good abrasion resistance. Robert Hadfield first produced the group in 1882; austenitic manganese steels are also called Hadfield Steels. The first known Hadfield steels contained 1.2 wt% Carbon and 12 wt% Manganese [38].

Being an alloy of iron, carbon, and manganese, the ideology behind using manganese as an alloying trusted element is to utilize its stabilizing property to delay the austenitic transformation of the FCC structure and assist in carbide formation. The ability of manganese and carbon to slow down phase transformations from austenite phase to martensitic phase makes this group

of steels suitable for engineering applications. Hence, it is essential to fix the correct percentage of raw materials of Mn and C to maintain phase stability and avoid early transformation. Amongst Mn and C, Mn has a significantly higher stabilizing ability. This steel group is widely used in cement, mining, and construction industries due to good flexibility, excellent resistance to wear such as gouging abrasion, high strength, and work hardening. These metals have lower initial yield strength; their work-hardening property complements this essential drawback. Work hardening is justified by transforming from δ to α to ε martensite due to strain, pseudo-twinning, dynamic strain aging, and interaction between dislocations with stacking faults [38] [39].

Through earlier studies, it was found that the formation of unfavorable amounts of carbides in grain boundaries is a possible cause of premature failures in this class of steel. It is often confusing to weigh in the advantages/ disadvantages of carbides, as a shortage in carbide formation leads to a loss of strength. Still, the excess can lead to phase instability, increasing brittleness, and the chance of fracture. (Fe, Mn)3C carbides and alpha ferrite carbides are known formations that create lamellae adjacent to the carbide network, leading to the depletion of carbon and Mn in the matrix adjacent to the carbide network. These adverse effects can be avoided by employing solution annealing treatment to remove the decarburized layer. Casting thickness plays a vital role in the properties possessed by the steel, as embrittlement of the cast is directly linked with embrittlement. Hardness in deeper layers of the cast Hadfield steel, compared to the layer that comes under mechanical contact, is lower due to the work hardening property during the test performed during the shot peening process [39] [40].

2.5 Niobium Carbide

Niobium carbide (NbC) is widely used to reinforce copper matrix composites and steel/iron-nickel for strengthening. It is used as the secondary phase of carbide to increase wear resistance, improve hot hardness, and limit grain growth. The hardness of niobium carbide is lower than that of titanium, tungsten, molybdenum, and chromium carbides [41] [42].

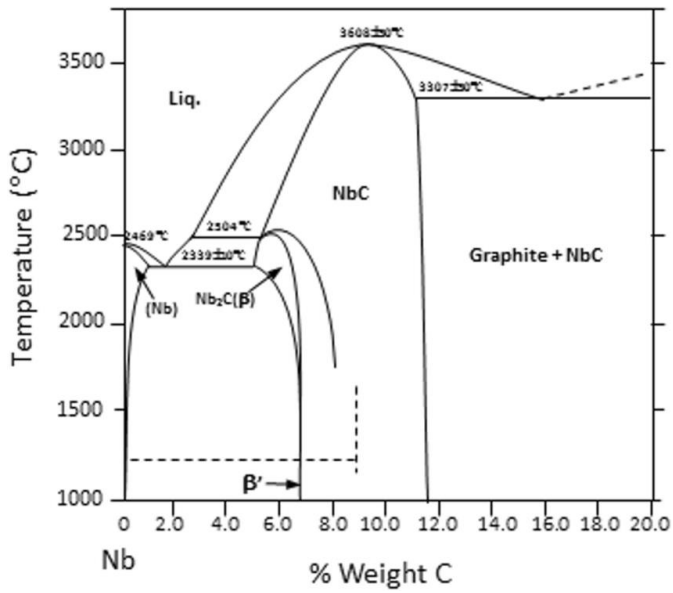

Figure 9: Binary phase diagram Nb-C [42]

In a preliminary analysis, NbC tools should outperform WC because, at 1225 °C, NbC is almost insoluble in Cr, Ni, Co, or Fe, whereas WC is completely soluble under the same conditions. Its high solubility in these metals causes the chemical wear (diffusion) of WC. According to Masalski, [43] NbC can form cubic sub-carbides, allowing for a wide range of carbon stoichiometry, as evidenced by the Nb-C binary phase diagram. Thus, Stoichiometry can be adapted to properties such as hardness and elasticity modulus in the NbC to $NbC_{0.75}$ range.

Vinitskii [42] investigated the C/Nb relationship and discovered that decreasing this ratio increases hardness while reducing the modulus of elasticity. In contrast to the binary phase diagram C/Nb, the W-C binary phase diagram shows a limited carbon content range to form the tungsten carbide used in cutting tool material. As a result, the production of WC powders is more difficult because the carbon must be added correctly to form tungsten carbide.

NbC is a NaCl-type face-centered cubic (FCC) structure crystal with lattice parameters of a = b = c = 0.4470 nm. Different growth kinetics, growth conditions, and growth mechanisms, on the other hand, can influence growth morphology [41]. Grove et al. [42] created NbC nanoparticles in situ by passing methane, ethylene, or acetylene gas through a plasma created by an arc discharge between two niobium electrodes. Moreover, the outcome resulted in NbC particles with various shapes. For instance, this experiment generated a cube with methane gas, a mixture of cube and cuboctahedron with ethylene gas, and cuboctahedron with acetylene gas [41].

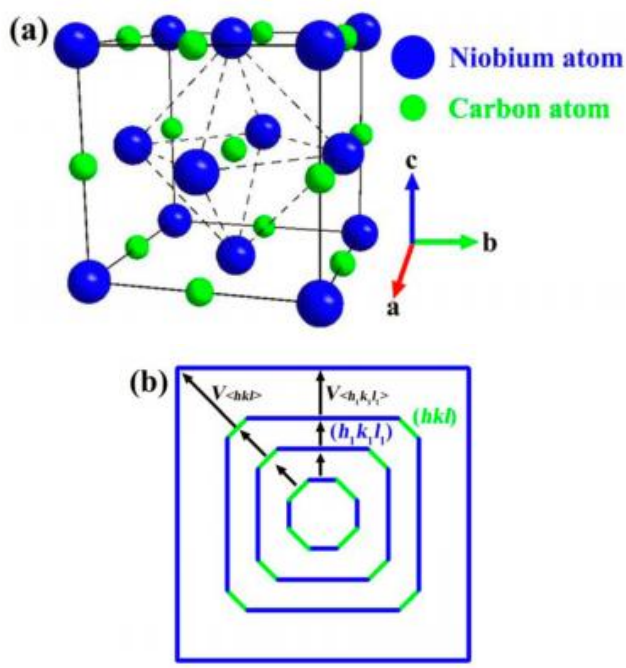

Figure 10: Graphical representation of (a) lattice structure of NbC (b)Crystal growth-outwards [41]

The variation in NbC particle morphology could be attributed to a change in carbon concentration, which altered the relative growth rate of the 111 and 100 faces on NbC crystals. However, the mechanical properties of NbC particles are heavily influenced by their shape and size. This is because NbC

particles of various morphologies are made up of faces with varying physical and chemical properties. The surface atom densities and chemical reactivity of faces 111, 110, and 100, for example, differ [41].

During the growth process, a cross-section of an octagonal crystal is shown in figure 12. As the crystal is growing, the facets with high surface energy (in green) eventually disappear. The facets with the least surface energy (in blue) influence the shape of the crystal resulting in a regular square crystal. [41].

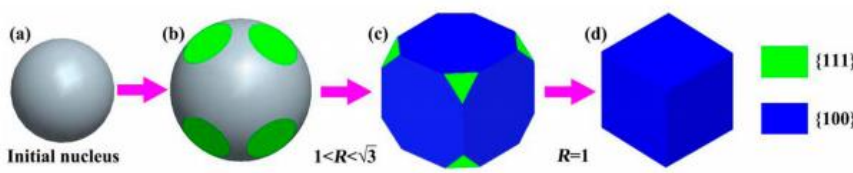

Figure 11: Morphology evolution in NbC [41]

Due to change in Nb/C ratio, there is a change in relative growth between {100} and {110} faces; this relative growth rate is termed as R; with this change in R, the shape of NbC deviates from its actual shape to other morphologies. If the relative growth between faces is one, the expected morphology is cuboidal [41].

3 Experimental Procedure

In this thesis, experiments will be carried out in the following sequence. After intensive research on the combinations of metals required for the MMC, the experiments will begin with mixing of samples, collection of samples to investigate it in (Energy Dispersive Spectroscopy) EDS to see if they have mixed homogenously; pressing the raw materials into samples; casting, heat treatment; cutting the samples for sample preparation followed by material characterization, finally wear testing.

After casting and heat treatment, the samples are cut and subjected to microstructural analysis. The best samples out of these are remanufactured

by following the same experimental flow. After their heat treatment, they are directly subjected to wear testing to see their performance.
Hence, the first set of manufacturing for microstructural characterization is batch 1; remanufacturing for wear testing is batch 2.

3.1 Classification of samples

While mixing the samples, there are high chances of contamination. Hence it is essential to rinse spatulas, bottles with acetone and let them dry before use.

Table 3: Classification of samples

Percentage	Class			
	N	**P**	**P-FM**	**P-FN**
*	N0	P0	-	-
**	N1	P1	PFM1	PFN1
***	N2	P2	PFM2	PFN2
****	N3	P3	PFM3	PFN3

The above table represents the categorization of the samples; here, two classes N and P are considered. The samples highlighted have not been made since there was a limitation of raw material. Hence these samples will be performed in future work.

After mixing, a sample of these powders was separated to conduct Scanning Electron Microscopy (SEM) analysis. The EDS analysis shows the powders' homogeneity; this shows that the above mixing conditions worked efficiently.

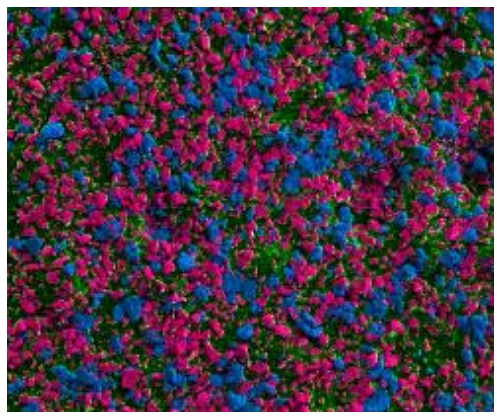

Figure 12: Represents homogenously mixed sample

A total of 16 samples mentioned in the above table are made for eight test plates, therefore two samples per test plate.

Table 4: Status of the samples after pressing

SNO.	Sample	Status of sample	Green density %
1.	N0	Very shallow cracks	84.75
2.	N1	Very shallow cracks	67.29
3.	N2	Very shallow cracks	65.78
4.	N3	Very shallow cracks	64.59
5.	P0	Very shallow cracks	69.98
6.	P1	Very shallow cracks	68.76
7.	P2	Very shallow cracks	62.31
8.	P3	One sample fractured other had shallow cracks	64.38
9.	P-FM1	Fractured into two pieces	65.47
10.	P-FM3	Very shallow cracks	65.27
11.	P-FN3	Very shallow cracks	59.4
12.	X	Completely cracked	-

3.2 Casting, Heat treatment

The samples are planned according to the casting design, each mold has a place for eight plates, and each plate has been accommodated with two samples, and the design is as shown fig 22,

Here plates 4,5 failed due to insufficient molten metal; the other samples with slight cracks are all macroscopic cracks which can be seen with the naked eye.
Hence, the total available samples are 8, i.e., N1, N2, N3 (2 samples), P1, P2, P3 (2samples).
The heat treatment cycle has been performed on these plates and the results as shown in table 7.

Table 5: Represents the status of plates after heat treatment

Sample	The result after heat treatment
N0	Cracks
N1	Slight cracks
N2	Slight cracks
N3	Both samples have slight cracks
P0	Cracked with a chip off
P1	No cracks, but the sample is fragmented
P2	Macroscopic pores
P3	sample are **perfect** despite a fracture in one during pressing
PFM1	No cracks but fragmented
PFM3	No cracks but fragmented
PFN1	Plate failure due to insufficient molten metal
x	Plate failure due to insufficient molten metal sample

After the heat treatment, all plates have been machined (grinded and polished) to eliminate sharp corners and irregularities. Since plate 8 with sample P3 (2 samples) looked fine after grinding and polishing, **plate 8 (P3) is saved for wear testing.** At the same time, other plates that had cracks and pores are further subjected to microstructural analysis.
Moreover, the plates are semi-cut and sent to LTH, where further cutting of samples is performed for sample preparation.

All these samples are hardened after heat treatment; hence, it takes 3-3.5hrs to cut out a single sample in the cut-off wheel machine. Hence a better solution was stacking all these plates one above the other and cutting them using wire-EDM; this alternative cuts with precision. The total time consumed is significantly less compared to the cut-off machine.
Before placing these samples in EDM, they have been stamped with codes for easy identification since all the samples look alike and get rusty after EDM.

Figure 13: Test plates stacked and being cut in Wire EDM

3.3 Sample Preparation

The rusty samples are to be prepared for microstructural analysis. A series of grinding and polishing steps are followed; the below-followed steps are the recommended steps.

However, the steps followed here are modified a bit based on the previous step, therefore after performing each grinding step, the sample was investigated in the microscope to see the improvement of the scratch, epoxy removal, etc.

The first step of sample preparation is the hot mounting, the mounting plate is dusted with antistick powder, and the sample is placed in the Citopress-5, Struers mount, and the most suitable resin for SEM is Polyfast, almost 13-15ml of fast poly resin is poured into the mounting cylinder, and the hot mount is begun, this process involves 3.5min of heating at 180C under 250 bar pressure and 1.5 min of cooling hence the total time involved is 5min for a 30mm sized mold.

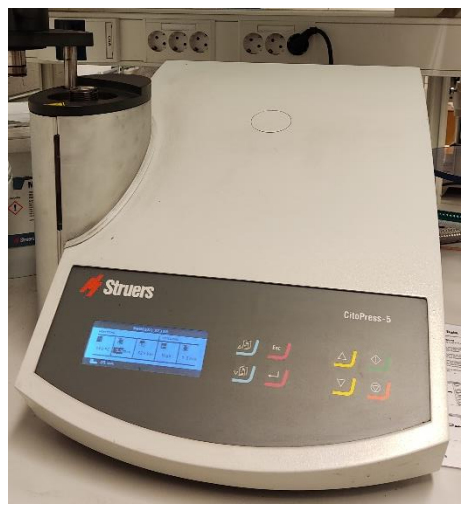

Figure 14: Struers Citopress 5 hot mounting equipment

The grinding tasks followed by polishing were easy to perform since all the steps followed are automated; it was difficult to start because of rusty samples. Hence, the rough grinding was performed under higher pressure while the rest were slightly lower pressure. It is important to note that using higher pressure will lead to uneven surfaces since the material removal rate of Hadfield steel will be higher than the NbC reinforcement.

Figure 15: Struers Tegramin 30 Grinding and Polishing equipment

The suspensions used for grinding is water; after every polishing step, the samples are thoroughly cleaned under running water and are wiped and dried

since the suspensions of each polishing step differ, and there is a risk that the suspension particles from one polishing step might stick onto the new polishing discs if they are not cleaned properly.

Table 6: Steps followed for grinding and polishing of samples

SNo	Disc	Suspension	Force N	Time (min)	Rotational speed (rpm)
1.	MD Piano 200	Water	40N	3.30	180
2.	MD Piano 500	Water	10N	8.30	180
3.	MD Piano 1200	Water	20N	5.30	180
4.	MD Piano 2000	Water	10N	3.30	180
5.	MD Piano 4000	Water	10N	3.00	180
6.	MD Dia	Diaduo (2-3)µm	10N	4.30	150
7.	MD Nap	Diaduo 1µm	5N	10.00	150
8.	MD Chem	OP U Non-dry	5N	5.00	150

3.4 Material Characterization

Due to time constraints, the possibility that all the samples can be analyzed under SEM is doubtful, hence to choose the best or better samples, Optical microscopy has been conducted on all the samples. The optical microscope used is Alicona at LTH; several images were taken at 2.5x, 20x, 50x, 100x. Later SEM is performed on four samples, and the equipment used is Tescan Mira 3 at the Department of Geology, Lund University.

3.5 Hardness test

After the microstructural analysis, the next step is to analyze the hardness results and correlate the particle size and hardness values. This thesis aims to improve the wear resistance and hardness of test plates; hence, to test this, hardness experiment has been performed on every sample; before this, it is to be made sure that the sample is clear without scratches. The equipment used here is a Vickers Microhardness tester; several indentations are made in both the matrix and reinforced regions through the transition region. Moreover, the average values of indents are considered as shown in the analysis section.

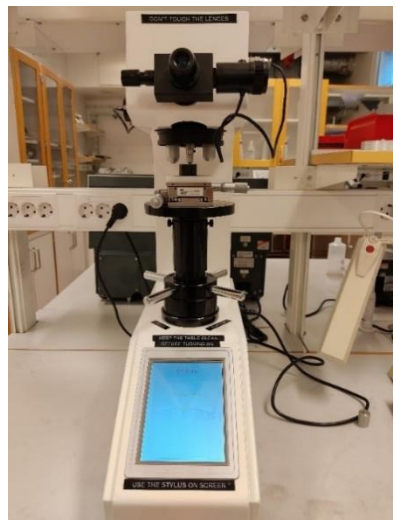

Figure 16: Vickers Micro Hardness tester

All the indentations are performed with 1kg load and a dwell time of 15s. Initially, the sample is to be placed on the holder; with the help of a microscope, the sample should be looked at and adjusted for making indents; creating several indents was a tedious task since the equipment is semiautomatic.

4. Analysis and discussion

4.1 Microstructural analysis

This image is an overview of all the samples taken in Alicona; the images have been converted to grayscale for better visual. In these images' cracks, pores, fragmented samples can be seen clearly.
The important things to determine during material characterization are,

- Draw a relation between microstructure, hardness, wear resistance
- the particle size of the NbC
- formation of cracks, pores
- look for the interface region between matrix and reinforcement, i.e., the transition region, to observe proper bonding.

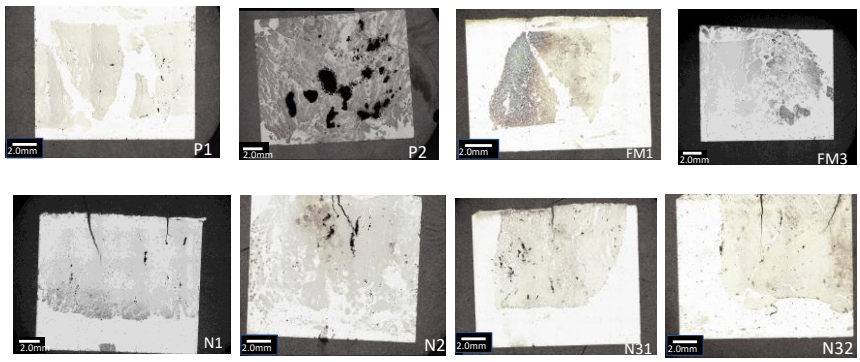

Figure 17: Overviews of samples captured in Alicona

For easy identification of two N3 Samples, they have been named N31, N32 but SEM analysis is performed only on one of them.
In the above sample overview images, samples FM1, FM3 are free of any macroscopic pores or cracks, while the rest of the samples possess macroscopic pores and cracks.

4.1.1. Reasons behind cracks, pores, fragmentation

Pores, cracks are the most commonly seen casting defects. Pores arise because of trapped air and the trapped air present could be because of improperly rammed mold, or sample, or during solidification process.

Cracks formed in the samples after heat treatment are different from the cracks obtained during pressing (cracks on N1, N2, N3 are all similar). However, the new cracks developed after casting during heat treatment since the coefficient of expansion for Hadfield steel and the reinforcement varies therefore cracks generate.

A significant observation for fragmentation is that the samples P2, FM3 were intact in one single piece with shallow cracks after pressing but can be seen that it was fragmented during casting, whereas FM1 fragmented in 2 pieces is held together by base alloy (manganese steel) two parts, as seen in the overview image *fig. 21*.

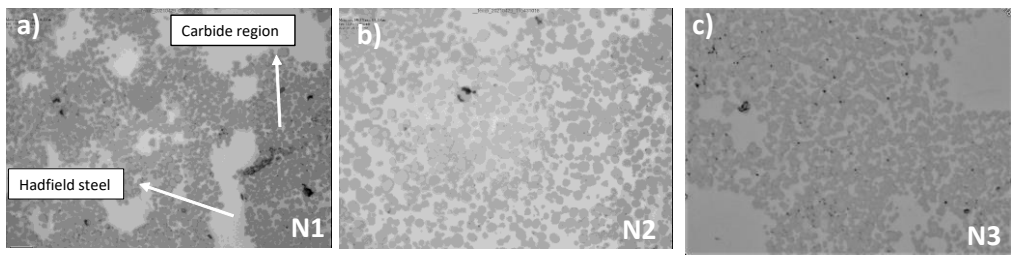

Figure 18: Alicona images of N1, N2, N3 show the reinforced particles amidst a pool of matrix (base alloy-Hadfield steel)

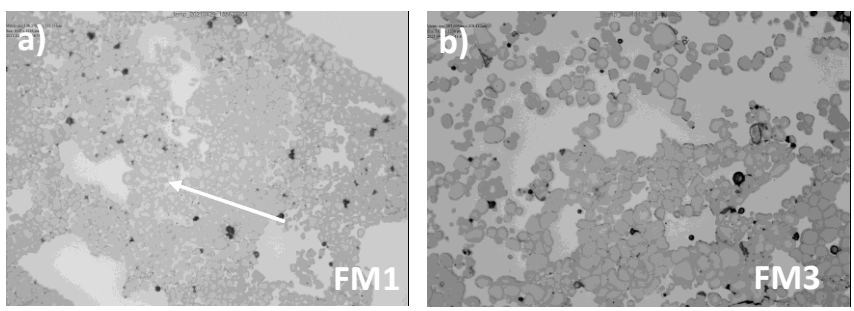

Figure 19: Alicona images of P1, P2 shows the reinforced particles amidst a pool of matrix (base alloy-Hadfield steel); the visible black spots are pores)

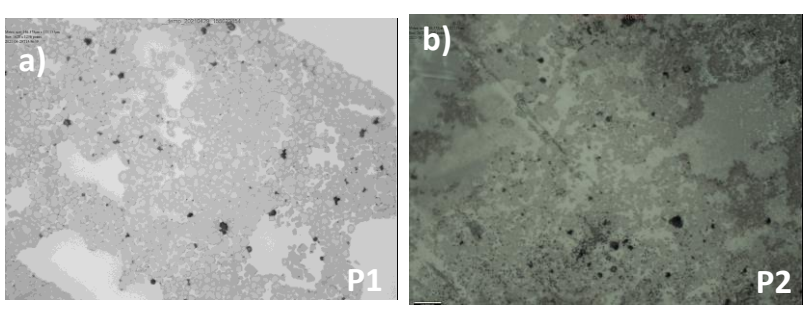

Figure 20: FM1, FM3, images from Alicona

All these images are captured at a similar magnification for easier comparison; all the samples show random distribution, and no particular

particle distribution pattern is found. Sample P2 was rusted after sample preparation since it collected sample preparation suspensions into its pores despite thorough cleaning with water and drying with N2 gun, P2 rusted eventually.
Amidst carbide particles, pools of Hadfield steel can be found. The particles shape in Alicona images seems to be globular or spheroidal, but analysis in SEM can give their morphology in detail.
These clusters of particles are not uniformly sized; the variation is very high; it can be seen that in all the samples, the particle size varies from the very smallest to the largest particle.

4.1.2. SEM analysis

The analysis is performed on Tescan Mira 3 in Geocentrum; due to time constraints and lab availability, only a few samples were analyzed, and they are P1, P2, N1, PFM1. This gives an excellent possibility to analyze the samples microstructure.

In general, the entire sample can be categorized into three regions, namely matrix, interface or transition region, and reinforced region; as discussed earlier, Hadfield steel is the matrix; NbC is the reinforcement, and the interface is the region between the matrix and the composite as shown in the below samples.

Moreover, it can be observed that there are no pores or cracks in N1, P1, P2 in the interaction zone. Hence it can be concluded that the bond between matrix and reinforcement is perfect. In FM1, pores are relatively high, and this is because the FM1 sample was broken and it was held together and cast; and it also can be said that the initial raw materials resulted in pore formation. When compared with P1, N1, N2, N3 do not have many pores as FM1, FM3.

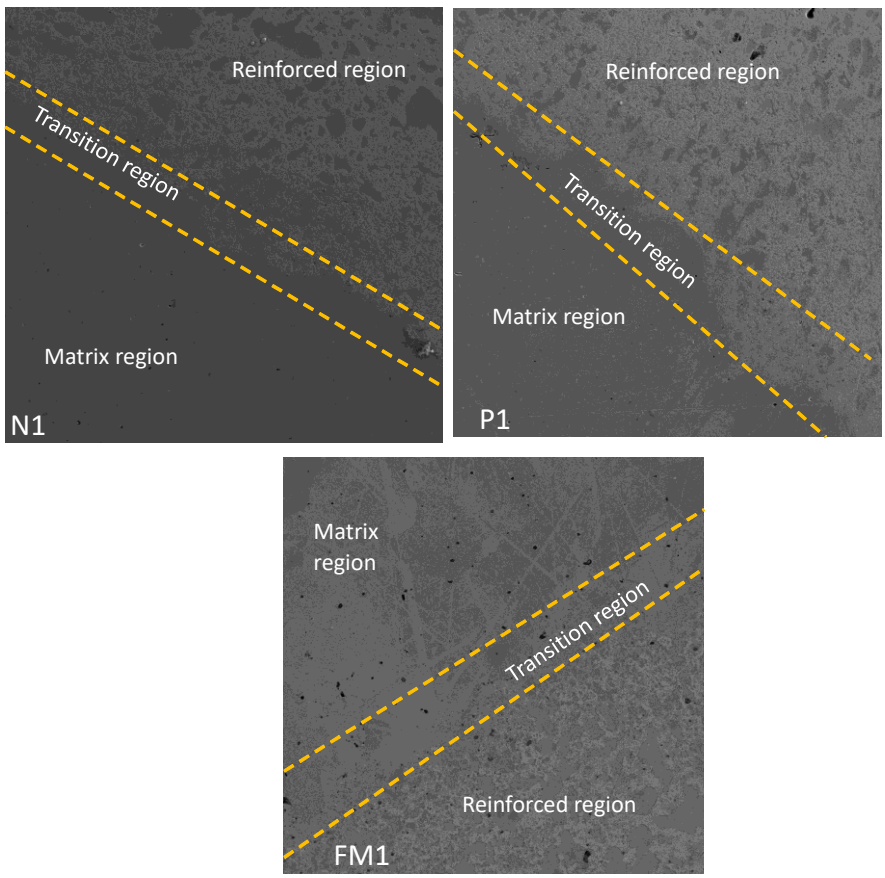

Figure 21: Clear visibility of variation in zones, matrix-Hadfield steel, reinforcement-NbC, transition- the interface between NbC and Hadfield steel

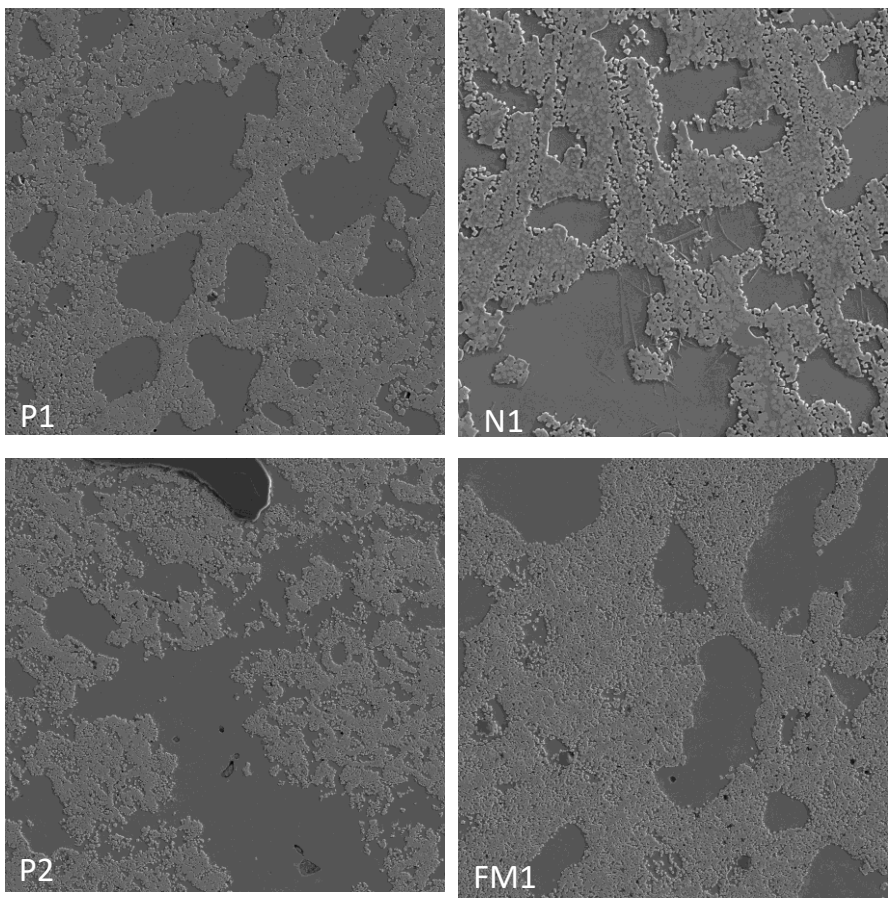

Figure 22: The above set of images represent FM1. N1, P1, P2 taken at similar magnification, and these images are captured inside the reinforcement region away from the interaction zone.

The above images are taken away from the interface region, which is inside the reinforced region. From all the images, it can be seen that the particle is not globular or spheroidal, but they are cuboidal; this is one of the morphologies of NbC.

Moreover, EDS analysis of a cuboidal particle confirmed that the particles are NbC. It was tested in a similar way for N2, P2, FM1, and all the analyzed have shown presence of NbC.

4.1.2.1. Comparison between samples

Average particle sizes of the samples have been determined, and the trend is as follows P1>P2>FM1>N1; the particle sizes of N1, FM1 seem to be pretty close.
Overall, the particle sizes of N1, P1, P2, FM1 are very close by with minute variation;

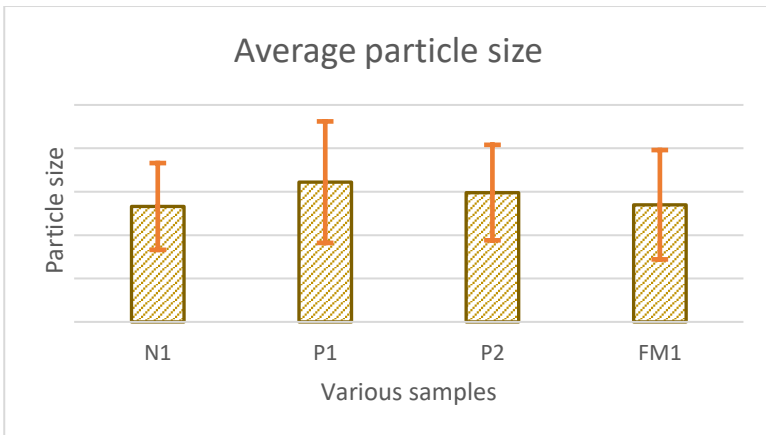

Figure 23: Graph representing average particle size of various samples

With increase in raw materials there is a decrease in particle size as can be seen between P1, P2.

4.2. Crack Deviation mechanism

This is one of the most toughness mechanisms possessed by composites, and it plays a predominant role. From the above-studied samples, some had pores and cracks (crack was found in FM1).

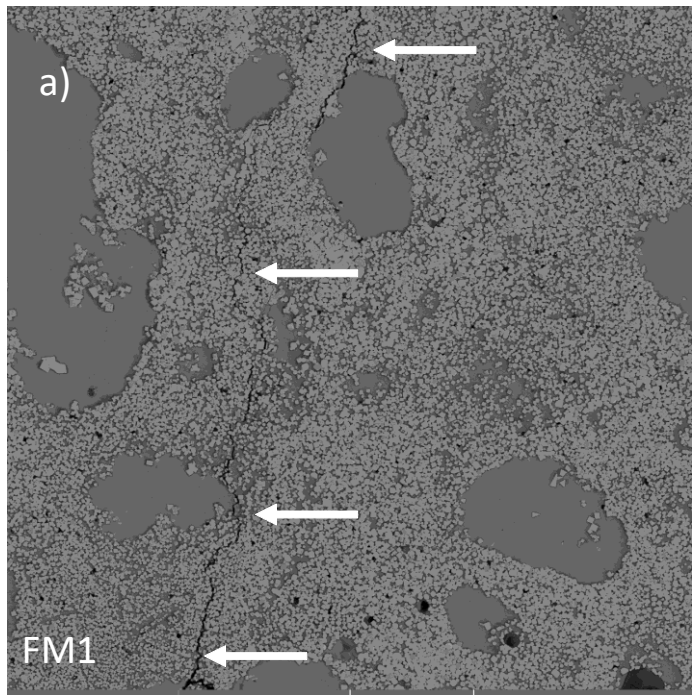

Figure 24: NbC particles deviate cracks

However, the samples reinforced with niobium carbide help in crack deviation, as shown above. This crack began, and instead of being a straight or a sharp crack just enough to break the sample when under impact, the crack deviates along the edges of the carbides preventing it from failure.

4.3 Different morphologies at the interface between molten metal and reinforcement

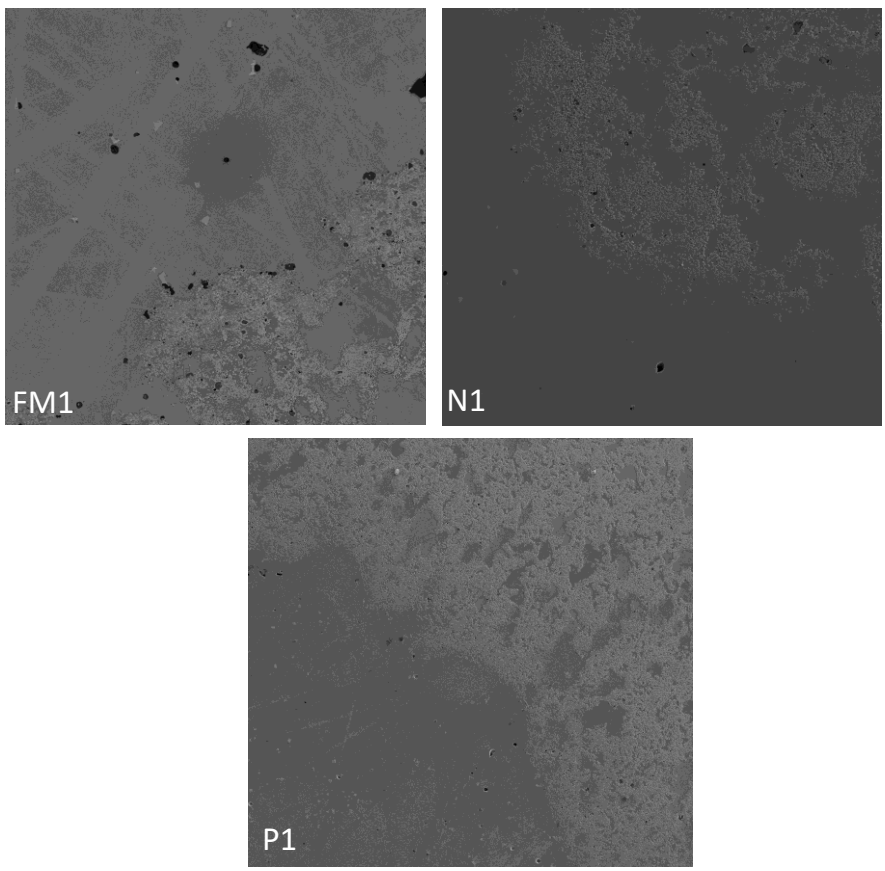

Figure 25: Images captured at the interface region

Compared to images in Figures 38, 40 the particle shape and size of NbC can be seen varying at the interface region. The reason behind this is that these particles are developed as a result of eutectic precipitation.

4.4 Effect of hardness on particle size

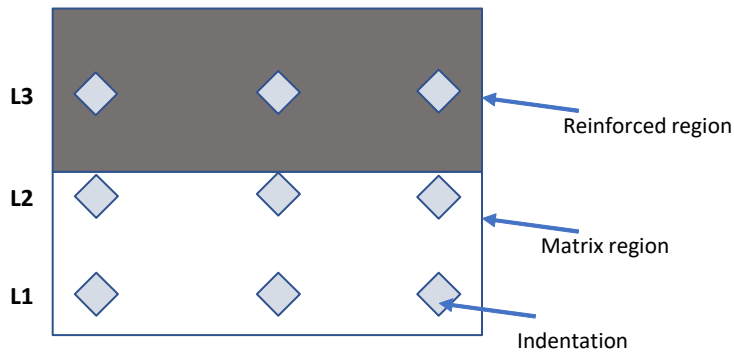

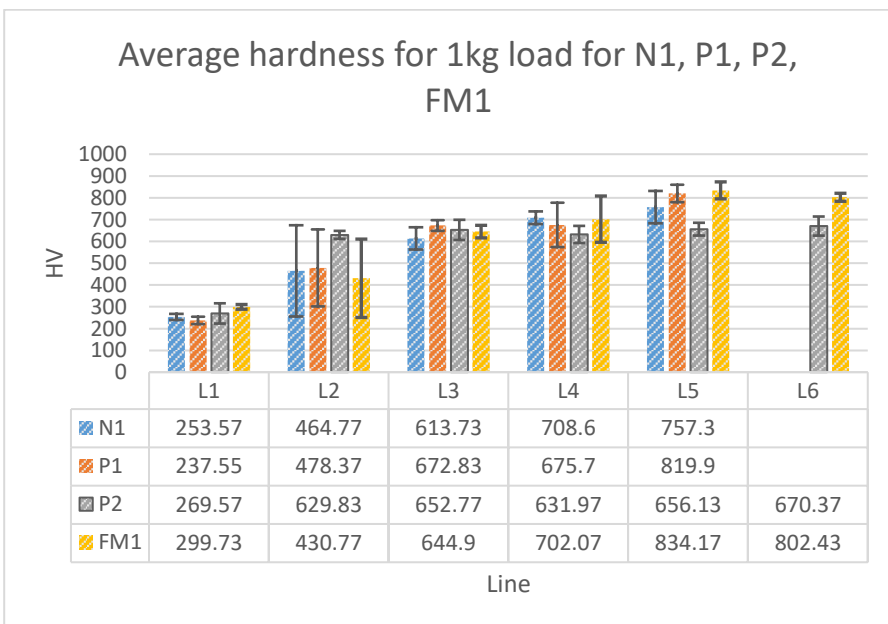

	L1	L2	L3	L4	L5	L6
N1	253.57	464.77	613.73	708.6	757.3	
P1	237.55	478.37	672.83	675.7	819.9	
P2	269.57	629.83	652.77	631.97	656.13	670.37
FM1	299.73	430.77	644.9	702.07	834.17	802.43

Figure 26: Graph representing average hardness of each line for each sample. Here X-axis represents Line 1, 2, 3…. And each line in each sample as shown above

Hence hardest sample among the SEM analyzed samples are FM1 despite its small particle size; this is majorly because of the effect of raw materials. Furthermore, the trend of the highest average hardness is FM1>P1>N1>P2. Between P1 and N1, P1 is the hardest, and among P1 and P2, P1 is the hardest. So, in this case, particle size is proportional to hardness; the more significant the particle size greater is the hardness.

The average hardness of the matrix region, i.e., the highest average hardness of the Hadfield steel calculated is 264HV; it can be observed that the hardness of the reinforced regions is almost three times the hardness of the non-reinforced region.

Similarly, hardness test has been performed on all the samples, and the overall highest average (only the highest averaged line value for every value is considered for comparison) values are made into a graph, and it looks as below,

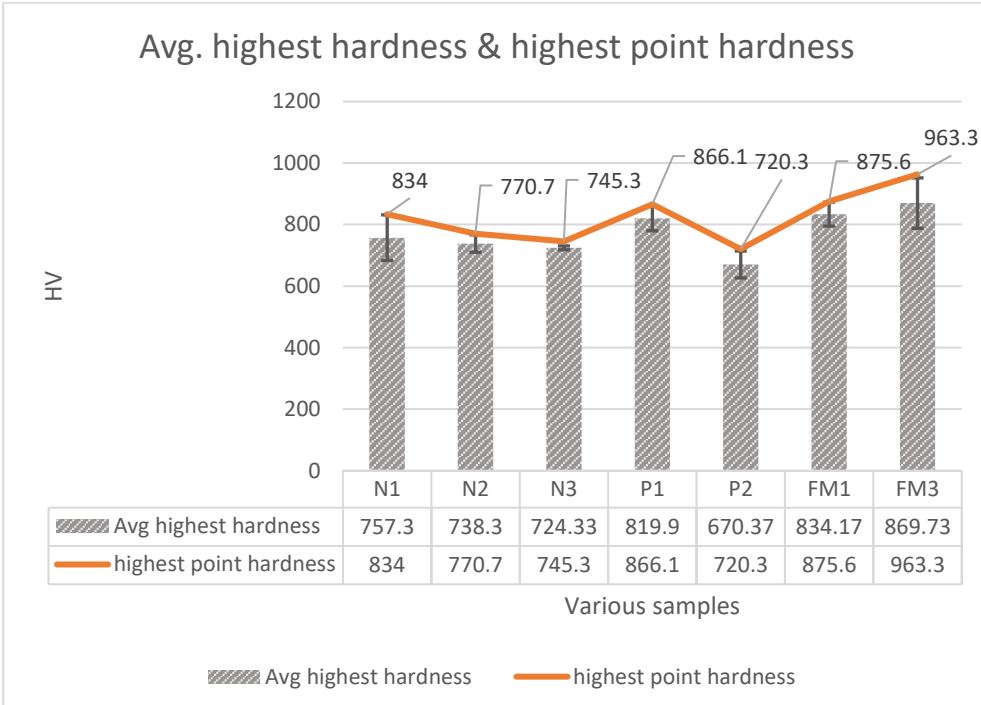

Figure 27: Graph representing variation between highest point hardness and average highest hardness in various sample

The highest average hardness has been found in sample FM3, and the trend follows as FM3 > FM1 > P1 > N1 > N2 > N3 > P2. Moreover, considering the trend of only the highest point hardness, it varies as FM3>FM1>P1>N1>N2>N3>P2.

The highest point hardness among the samples is FM3, i.e., 963.3HV, but its average falls to 869.73HV. Therefore, the standard deviation is high, indicating the values have too much variation.

Considering the highest point hardness, the hardness of reinforced is at least 3.6 times higher than the non-reinforced region.

4.5 Wear test

Since the batch-1 plates are cut out for microstructural investigation, a new set of plates will be manufactured specifically for wear testing. To

manufacture these, similar sets of steps are followed as before, starting from powder processing until casting the sample. Hence a similar casting design as batch-1 is followed.

It has been decided that P1, P2, N1, and P3 will be made for the wear test. Only Plate 4 (of two P3 samples) was tested for wear.
Hence the first set of wear tests is performed on P3 sample. Usually, wear can be measured by material loss. Hence the test was performed with 4 tonnes of rock mixture.

All four plates are weighed before and after wear testing in each step to determine weight loss. From this, weight loss volume loss is derived from which wear ratio is calculated.

Here, after crushing 1ton of rocks, there is a significant volume loss of the plates, and the volume loss increased after crushing 2 tons of rocks. However, there is a reduction in volume loss after crushing 3 tons of rocks, and the wear ratio remained the same after crushing 4 tons of rocks; this shows that Hadfield steel has work-hardened, and the material loss is curbed. After examining the plates after each test, it was observed that the reference plates had undergone severe wear damage, while the test plates have not undergone such severe wear.

Table 7: Results of P3 from wear testing.

Sample name	Wt. of rocks (Kg)	F=Wear ratio
P3	1000	0.23
	2000	0.25
	3000	0.24
	4000	0.24

This volume loss is the loss of material on the Hadfield steel due to gouging abrasion, but this gouging abrasion has not impacted the NbC reinforcement region.
Hence P3 successfully worked, therefore reinforcing test plates with NbC derived good results.

5. Conclusion

This new research on reinforcing Hadfield steel with Niobium carbide is successful on the studied test plates,

- The hardness of the reinforced region is higher than the hardness of the non-reinforced region.
- Through the analysis, it was found that the effect of slightly varying raw materials result in several microscopic changes like particle size, which indeed impact the sample's hardness.
- And through microstructural and mechanical investigation, it is found that hardness increases with increase in particle size.

6. Future Scope

Since the conditions are satisfactory, there is much scope for improvising this project for future work.

- Due to time constraints, only four samples were analysed in SEM. Hence the remaining samples should be further analysed.
- Another vital aspect is XRD analysis; due to limited access, this analysis could not be carried out; hence, it is highly suggested to carry out XRD analysis in analysing formed phases.
- Though batch two plates are manufactured, there was not enough time to wear test all the samples, hence this can be further carried out.

7. Bibliography

[1] K. Chawla, ”Metal matrix composites. In Composite Materials,” i *springers*, New York, NY., 2012.

[2] S. a. M. Z. Tjong, ”Microstructural and mechanical characteristics of in situ metal matrix composites.,” *Materials Science and Engineering: R: Reports,,* vol. 29, nr 3-4, pp. 49-113, 2000.

[3] S. Rawal, ”Metal-matrix composites for space applications.,” *springer*, vol. 53, nr 4, pp. 14-17, 2001.

[4] E. a. P. A. Prusov, ”Properties of cast aluminum-based composite alloys reinforced by endogenous and exogenous phases,” *Russian Metallurgy (Metally)*, pp. 670-674, 2011(7).

[5] M. S. L. B. B. I. a. H. A. Coteață, ”Analysis of EDM drilling of porous SiC/Al-Mg composite.,” *In AIP Conference Proceedings, AIP Publishing LLC*, vol. 2113 No 1, 2019.

[6] T. a. W. P. Clyne, An introduction to metal matrix composites., Cambridge university press., 1995.

[7] M. a. Z. X. Tan, ”Powder metal matrix composites: selection and processing,” *Materials Science and Engineering: ,* vol. 244, nr 1, pp. 80-85, 1998.

[8] D. E. B. M. a. H. M. Huda, ”Metal-matrix composites: Materials aspects. Part II.,” *Journal of Materials Processing Technology, ,* vol. 37, nr 1-4, pp. 529-541., 1993.

[9] Y. Nishida, introduction to Metal Matrix Composites: Fabrication and Recycling., Springer Science & Business Media., 2013.

[10] P. S. S. a. P. H. Bains, ”Fabrication and machining of metal matrix composites: a review.,” *Materials and Manufacturing Processes,,* vol. 31, nr 5, pp. 553-573, 2016.

[11] X. Tong, ”Metal Matrix Composites,” i *Advanced Materials by Design*, CRC press, 2016, pp. 1-21.

[12] W. Harrigan Jr, ”Commercial processing of metal matrix composites.,” *Materials Science and Engineering:,* vol. 244, nr 1, pp. 75-79, 1998.

[13] L. CHYUAN, ”Linear Static Finite Element Analysis of Composite Hat-stiffened Laminated Plates (Doctoral dissertation, Universiti Teknologi Malaysia),” 2005.

[14] N. a. S. S. Kumar, ”Selection of reinforcement for Al/Mg alloy metal matrix composites.,” *Materials Today: Proceedings, ,* vol. 21, pp. 1605-1609., 2020.

[15] M. a. M. H. Woydt, ”The use of niobium carbide (NbC) as cutting tools and for wear resistant tribosystems.,” *international Journal of Refractory Metals and Hard Materials,,* vol. 49, pp. 212-218, 2015.

[16] M. a. S. S. 2. Cuppari, ”Physical properties of the NbC carbide.,” *Metals,,* vol. 6, nr 10, p. 250, 2016.

[17] Y. a. P. P. Kryl, ”Structure formation and properties of NbC-Hadfield steel cermets. Structure formation and properties of NbC-Hadfield steel cermets.,” *Journal of Superhard Materials,,* vol. 35, nr 5, pp. 292-297, 2013.

[18] L. S. J. K. B. L. S. J. S. W. Z. a. W. X. Wang, ” Electrochemical behaviour and surface conductivity of niobium carbide-modified austenitic stainless steel bipolar plate.,” *Journal of power sources,* vol. 246, pp. 775-782., 2014.

[19] M. M. H. V. J. a. H. S. Woydt, ”Niobium carbide for wear protection–tailoring its properties by processing and stoichiometry,” *Metal Powder Report,* vol. 71, nr 4, pp. 265-272., 2016.

[20] E. H. D. K. K. M. P. P. L. a. W. M. Uhlmann, ”Increased tool performance with niobium carbide based cutting materials in dry cylindrical turning.,” *Procedia CIRP,,* vol. 77, pp. 541-544., 2018.

[21] B. Roebuck, Nature and Properties of Refractory Carbides. Powder Metallurgy, 2001, 44(1), p.14.

[22] K. J. H. a. V. L. Q. Zhang, ”Production methods of ceramic-reinforced Al-Li matrix composites: A review.,” *Journal of Composites and Compounds,* vol. 2, nr 3, pp. 77-84, 2020.

[23] B. Y. H. a. L. W. Ralph, ”The processing of metal matrix composites—an overview.,” *Journal of materials processing technology,* vol. 63, nr 1-3, pp. 339-353, 1997.

[24] B. K. J. a. S. H. Kandpal, ”Manufacturing and technological challenges in stir casting of metal matrix composites–a review.,” *Materials Today: Proceedings,* vol. 5, nr 1, pp. 5-10., 2018.

[25] A. M. B. P. L. a. d. J. Soares, ”Thermal expansion behaviour of magnesium boron fibrous composites,” *International Journal of Vehicle Structures & Systems,* vol. 4 (4), p. 148, 2012.

[26] B. Sunil, ”Developing Surface Metal Matrix Composites: A Comparative Survey.,” *International Journal of Advances in Materials Science and Engineering (IJAMSE)* , vol. 4, nr 3, 2015.

[27] R. Everett, ”Deposition technologies for MMC fabrication (pp. 103-119),” i *Academic Press, Harcourt Brace Jovanovitch, San Diego, CA, USA.* , San Diego, CA, USA. , 1991.

[28] A. M. J. G. K. K. W. a. P. D. Śliwa, ”Internal stresses in PVD coated tool composites.,” *Archives of Metallurgy and Materials,* vol. 61, 2016.

[29] S. S. P. M. M. a. R. M. Sakthivelu, ”Synthesis of metal matrix composites through stir casting process-a review.,” *Mechanics and Mechanical Engineering,,* vol. 22, nr 1, pp. 357-370., 2020.

[30] M. B. S. a. V. M. Kumar, ”Influence of stir casting parameters on particle distribution in metal matrix composites using stir casting process.,” *Materials Research Express,,* vol. 6, nr 10, p. 1065d4., 2019.

[31] A. S. S. V. A. a. K. B. Pal, ”Stir Casting of Metal Matrix Composites–A Review.,” *International Journal of Computer & Mathematical Sciences,,* vol. 4, 2015.

[32] S. R. S. a. S. S. Thandalam, ”Synthesis, microstructural and mechanical properties of ex situ zircon particles (ZrSiO4) reinforced Metal Matrix Composites (MMCs),” *Journal of Materials Research and Technology,* vol. 4 (3), pp. 333-347, 2015.

[33] M. a. K. V. Dhanashekar, ”Squeeze casting of aluminium metal matrix composites-an overview.,” *Procedia Engineering,* vol. 97, pp. 412-420., 2014.

[34] R. Bhagat, ”High pressure squeeze casting of stainless steel wire reinforced aluminium matrix composites. Composites,” vol. 19, nr 5, pp. 393-399, 1988.

[35] P. S. N. a. R. C. Madhukar, ”Manufacturing of aluminium nano hybrid composites: a state of review.,” i *In IOP Conference Series:Materials Science and Engineering; Vol. 149, No. 1, p. 012114*, 2016.

[36] J. M. M. a. P. P. Gohil, ”Research review of diversified reinforcement on aluminum metal matrix composites: Fabrication processes and mechanical characterization,” *Sci. Eng. Compos. Mater,* vol. 25(4), p. 633–647, 2018.

[37] J. a. G. P. Mistry, ”An overview of diversified reinforcement on aluminum metal matrix composites: Tribological aspects.,” *Proceedings of the Institution of Mechanical Engineers, Part J: Journal of Engineering Tribology,,* vol. 231(3), pp. 399-421., 2017.

[38] W. a. H. C. Bleck, ”Physical metallurgy of high manganese steels.,” *mdpi,* 2019.

[39] A. a. D. K. Srivastava, ”Microstructural characterization of Hadfield austenitic manganese steel.,” *Journal of Materials Science, ,* vol. 43, nr 16, pp. 5654-5658., 2008.

[40] E. a. C. Y. Astafurova, ”Strain hardening upon twinning of $$[\bar 111],[\bar 144] $$, and [011] single crystals of hadfield steel. The Physics of Metals and Metallography,,” *The Physics of Metals and Metallography, ,* vol. 108, nr 5, pp. 510-518, 2009.

[41] H. Z. L. W. J. L. Z. a. X. Y. Bai, ”Morphological evolution of NbC particles at the interface of niobium–iron diffusion couple.,” *Materials Science and Technology,,* vol. 36, nr 16, pp. 1749-1755, 2020.

[42] L. S. R. B. G. R. D. a. B. A. Fernandes, ”Influence of sintering condition on the tool wear of NbC-based Ni binder-cemented carbide cutting tools.,” *The*

International Journal of Advanced Manufacturing Technology, , vol. 106, nr 7, pp. 3575-3585., 2020.

[43] R. Cahn, ”Binary alloy phase diagrams–second edition.,” *ASM international, Materials Park, Ohio, USA*, vol. 3, p. 3589, 1991.

[44] J. X. Y. Q. W. a. H. R. Jiang, ”Important factors affecting the gouging abrasion resistance of materials.,” *Minerals Engineering,* Vol. %1 av %2238-246., pp. 238-246., 2018.

[45] V. a. B. R. Golovanevskiy, ”Gouging abrasion test for rock abrasiveness testing.,” *International Journal of Mineral Processing,*, vol. 85, nr 4, pp. 111-120., 2008.

[46] s. engineering, ”Abrasion,” [Online]. Available: https://surfaceengineering.com/wear-modes/abrasion/. [Använd March 06 2021].

[47] Y. a. L. W. Dastur, ”Mechanism of work hardening in Hadfield manganese steel.,” *Metallurgical transactions A,* , vol. 12, nr 5, pp. 749-759., 1981.